Corpora amylacea act as containers that remove waste products from the brain

Marta Riba[a,b,c,1], Elisabet Augé[a,b,c,1], Joan Campo-Sabariz[a,d], David Moral-Anter[a,d], Laura Molina-Porcel[e], Teresa Ximelis[e], Ruth Ferrer[a,d], Raquel Martín-Venegas[a,d], Carme Pelegrí[a,b,c,2], and Jordi Vilaplana[a,b,c,2]

[a]Secció de Fisiologia, Departament de Bioquímica i Fisiologia, Universitat de Barcelona, 08028 Barcelona, Spain; [b]Institut de Neurociències, Universitat de Barcelona, 08035 Barcelona, Spain; [c]Centros de Biomedicina en Red de Enfermedades Neurodegenerativas (CIBERNED), 28031 Madrid, Spain; [d]Institut de Recerca en Nutrició i Seguretat Alimentàries (INSA-UB), Universitat de Barcelona, 08291 Barcelona, Spain; and [e]Neurological Tissue Bank of the Biobanc-Hospital Clinic-Institut d'Investigacions Biomèdiques August Pi i Sunyer (IDIBAPS), 08036 Barcelona, Spain

Corpora amylacea (CA) in the human brain are granular bodies formed by polyglucosan aggregates that amass waste products of different origins. They are generated by astrocytes, mainly during aging and neurodegenerative conditions, and are located predominantly in periventricular and subpial regions. This study shows that CA are released from these regions to the cerebrospinal fluid and are present in the cervical lymph nodes, into which cerebrospinal fluid drains through the meningeal lymphatic system. We also show that CA can be phagocytosed by macrophages. We conclude that CA can act as containers that remove waste products from the brain and may be involved in a mechanism that cleans the brain. Moreover, we postulate that CA may contribute in some autoimmune brain diseases, exporting brain substances that interact with the immune system, and hypothesize that CA may contain brain markers that may aid in the diagnosis of certain brain diseases.

corpora amylacea | meningeal lymphatic system | aging | phagocytosis | natural immune system

In 1837 the anatomist and physiologist J. E. Purkinje described the presence of some particular granular bodies in the brain of elderly patients (1). Virchow, in 1854, described them in more detail and observed that these bodies (*corpora* in Latin) share some similarities with starch (*amylum* in Latin) (2). These bodies, named *corpora amylacea* (CA), were initially considered to have no pathological significance and for a long time were thought to be irrelevant. In recent decades, however, this perception has changed. With the advances in technology, CA have been studied from different perspectives and a large number of theories regarding their nature have been put forward. Unfortunately, none of these theories have been demonstrated conclusively and CA remain intriguing and mysterious bodies. In the present study, several features of CA are described and a vision of their function is proposed which may have implications for clinical practice.

There is a consensus that the main components of CA are polymerized hexoses (primarily glucose) (3) and it has been estimated that hexoses constitute about 88% of their weight (4). Along with polymerized hexoses, other components originating in neurons, astrocytes, or oligodendrocytes, from blood or of fungal or viral origin, have also been described, although some of them have generated controversy (5). In 2017 we reported that CA contain neoepitopes that are recognized by natural antibodies of the immunoglobulin M (IgM) isotype (6). We also observed that these IgMs were present as contaminants in numerous commercial antibodies used for immunohistochemistry procedures and, since these contaminant IgMs are recognized by the majority of the secondary antibodies, they frequently cause false positive immunostaining in CA. These IgMs therefore account for some of the inconsistencies concerning CA composition and are the main reason for the uncertainty surrounding their origin and functions. In subsequent work, we reviewed the presence of the components previously described in CA and were able to rule out some of them, at least at levels that can be detected by immunohistochemistry (5,

6). Nonetheless, we observed that CA contain glycogen synthase (GS), an indispensable enzyme for polyglucosan formation, and also ubiquitin and protein p62, both associated with processes of elimination of waste substances (5). The relationship between CA and waste substances is recurrent in the literature. Already in 1999, after a detailed and complete review, Cavanagh indicated that "CA functions seem to be directed towards trapping and sequestration of potentially hazardous products of cellular metabolism, principally derived from the aging process, but probably also from any disease state resulting in excessive amounts of potentially harmful metabolic products" (3). Although some of these hazardous products were described after carrying out unreliable immunohistochemical procedures, the results obtained using other techniques have supported their presence. In this regard, ultrastructural studies by Sbarbati et al. (7) indicated that CA originate in astrocytes and accumulate abnormal material, and the study by Augé et al. (8) showed that CA are formed inside astrocytes by the accumulation of residual products, including degenerating mitochondria and membranous fragments originating from degenerative processes. Moreover, combining the results of human neuropathological surveys, cell culture techniques, and animal models, some authors have proposed that CA are homologous to "Gomoripositive" granules which accumulate in subcortical/periventricular regions of the rodent brain and which are derived from damaged

Significance

Aging and neurodegenerative processes induce the formation of waste substances in the brain. Some of these substances accumulate in *corpora amylacea* (CA). We reveal that CA are released from the brain into the cerebrospinal fluid and are present in the cervical lymph nodes, into which cerebrospinal fluid drains through the meningeal lymphatic system. We also show that CA can be phagocytosed by macrophages. We conclude that CA can act as waste containers and hypothesize that CA are involved in a mechanism that cleans the brain. We also postulate that CA may contain clinical markers of brain disorders and may also play significant roles in some brain autoimmune diseases. These last points merit further study due to their possible clinical implications.

[1]M.R. and E.A. contributed equally to this work.

[2]To whom correspondence may be addressed. Email: carmepelegri@ub.edu or vilaplana@ub.edu.

mitochondria engaged in a complex macroautophagy process (9, 10). For their part, using a combination of 2D electrophoresis with matrix-assisted laser desorption/ionization time-of-flight mass spectrometry, Selmaj et al. (11) identified several proteins of suspected neuronal origin and others involved in the regulation of apoptosis and senescence, supporting the notion that the biogenesis of CA involves the degeneration and aggregation of substances, some of them of neuronal origin. Moreover, Cissé et al. (12) already described the presence of ubiquitin in CA in high-performance liquid chromatography (HPLC) studies. Taken together, this evidence indicates a relationship between CA and waste elements and reinforces the idea that CA are waste containers formed by a polyglucosan structure that amasses waste products (6).

It is well known that CA are located mainly in perivascular, periventricular, and subpial regions of the brain (4). Since the glymphatic system drains the interstitial fluid (ISF) from the perivascular regions to the cerebrospinal fluid (CSF) (13), and since both periventricular and subpial regions are close to the cavities that contain the CSF (i.e., ventricles and subarachnoid space), it is plausible that, as several authors have proposed, CA are expelled from the brain to the CSF (3–7, 14). In biopsied material from the vestibular root entry zone in cases of Ménière's disease, Sbarbati et al. (7) observed at ultrastructural level that CA were sited in astroglial processes of the glia limitans, near the pial region. Around these CA the astrocytic cytoplasmic membrane presents folds that create fissures which, according to these authors, may split the CA apart, allowing them to escape into the pial connective tissue or subpial space. In this regard, in a study with human hippocampal tissue, we observed the presence of CA in both the subependymal region and beneath the pia and, occasionally, inside the CSF of the ventricular region. This evidence (summarized in Fig. 1) seems to indicate a possible route of escape for the CA into the CSF.

The CSF drains not only via arachnoid granulations, as classically believed, but also via the recently rediscovered meningeal lymphatic system (15). The presence of lymphatic vessels collecting CSF at the base of the skull was described for the first time by Földi et al. (16). Johnston et al. (17) reported connections between the CSF and nasal lymphatic vessels in humans and other mammals. Later, lymphatic vessels collecting CSF were also described lining the dural sinuses by Louveau et al. (18, 19), and new techniques based on magnetic resonance imaging permit their in vivo visualization (20). From meningeal lymphatic vessels and subsequent lymphatic vessels, lymph crosses different cervical lymph nodes (18, 21) before accessing the lymphatic duct or right thoracic duct, which ultimately drain into the brachiocephalic veins. The images in Fig. 2 sketch the structure of the meninges, including the meningeal lymphatic system, as well as the routes of the lymphatic vessels that descend to the neck and cervical lymph nodes. On this basis, it has been reported that meningeal lymphatic vessels allow the brain to eliminate macromolecules by collecting them from the CSF (22). Conceivably, in the same way as waste molecules generated in the brain, it is possible that CA released from the brain into the CSF escape from the CSF via the meningeal lymphatic system, reaching the deep cervical lymph nodes or beyond. The lymphatic capillaries are formed by overlapping cells that can act as valves leaving relatively large openings, allowing the passage of macromolecules and even cells, and thus also the passage of CA.
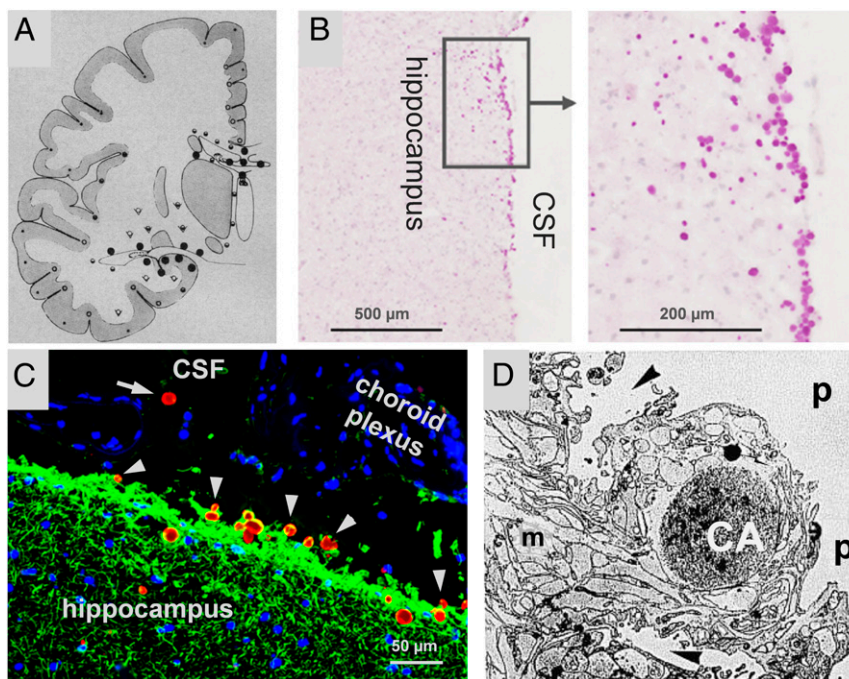
Fig. 1. Distribution of CA in human brain and possible extrusion into the CSF. (*A*) Distribution of CA in cerebrum of 70-y-old brains (· rare, ∘ occasional, ☙ common, ● extremely rich, ⌄ variable). Note that CA tend to be concentrated in the proximity to CSF (mean from 4 cases). Adapted with permission from ref. 4. Copyright 1969 American Medical Association. All rights reserved. (*B*) Hippocampal section of human brain stained with PAS. CA (magenta spots) can be observed in the border of the hippocampus. Adapted with permission from ref. 5, which is licensed under CC BY 4.0. (*C*) Hippocampal section of human brain stained with α-glial fibrillary acidic protein (α-GFAP) (green), mouse IgMs directed against neoepitopes (red), and Hoechst (blue). Note that almost all CA (stained with the IgMs) are partially encircled with astrocytic fibrils (stained with α-GFAP). Clustered nuclei (blue staining) in the ventricle are from cells from choroid plexus. Some CA seem to escape from hippocampus (arrowheads) and one is located inside the ventricle (arrow), all suggesting that CA can be extruded from brain. (*D*) Proposed extrusion of CA at the vestibular root entry zone. The CA is generated inside the astrocyte and, after the formation of a system of ramified scissurae around the CA, it is transferred to the pial connective tissue. m, marginal glia; p, pial connective tissue; arrowheads, scissurae on astrocyte enveloping the CA. Original image: 3,100×. Adapted from ref. 7 by permission of Oxford University Press.
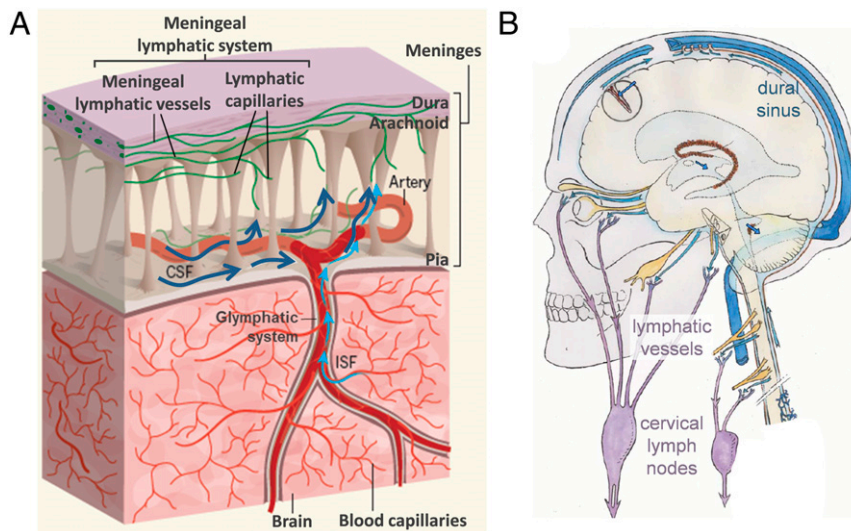
Fig. 2. Drainage of CSF via the meningeal lymphatic system. (*A*) Part of the CSF drains from the subarachnoid space via the lymphatic meningeal system. In turn, ISF drains to the subarachnoid space via the glymphatic system. These routes allow the elimination of waste elements and macromolecules generated in the brain tissue. Adapted by permission from ref. 22, Springer Nature: *Nature*, copyright 2018. (*B*) The meningeal lymphatic vessels descend to the neck, where the cervical lymph nodes are located. These nodes are involved in the elimination of waste products (the scheme does not depict the lymphatic vessels lining the dural sinuses). Adapted from ref. 23. Copyright 2011 Elsevier Masson SAS. All rights reserved.

As we indicated in previous work, CA contain neoepitopes that are recognized by natural IgM antibodies (6). Natural IgM antibodies are generated even before birth, without exposure to external antigens, and contribute to critical innate immune functions such as the maintenance of tissue homeostasis (24). Carbohydrate epitopes are targets of immune surveillance and natural IgM antibodies (25, 26). Some of these epitopes are generated de novo under triggering circumstances in cells or structures of the body itself, and are thus known as neoepitopes. For instance, in aging processes there is an increase in the generation of advanced glycation end products (27), which can act as neoepitopes, and neoepitopes of carbohydrates have also been described in malignant tumor cells (26, 28). In the case of CA, the interaction between IgMs and neoepitopes cannot occur inside the brain, because CA are intracellular structures and thus have a limiting membrane (7, 8). Moreover, IgMs do not cross the blood–brain barrier and so do not have access to the brain parenchyma or the CSF (6). Hence, if CA are extruded from the brain to the CSF and reach the cervical lymph nodes via the meningeal lymphatic vessels, their interaction with IgMs may take place in the cervical lymph nodes. Furthermore, since phagocytosis is one of the responses triggered by natural IgMs, it would be interesting to examine whether lymph node macrophages can phagocytose them. It must be pointed out that CA being phagocytosed by macrophages has been observed in samples from cases of neuromyelitis optica, a condition that involves tissue inflammation, vascular alterations, and probably the disruption of the blood–brain barrier (29).

Overall, this evidence suggests a mechanism for eliminating residual substances from the brain in which CA act as waste containers that are extruded from the brain to the CSF. Afterward, via the meningeal lymphatic system, CA can reach the cervical lymph nodes, and macrophages located there may play a significant role in their phagocytosis. We therefore studied the possible presence of CA in the CSF, their presence in the cervical lymph nodes, and their interactions with macrophages.

Results

CSF Contains CA. To study the presence of CA in the CSF, we analyzed several CSF samples supplied by the Biobanc-Hospital Clinic-Institut d'Investigacions Biomèdiques August Pi i Sunyer (IDIBAPS). According to the standard protocol used at this facility, samples are centrifuged at $4{,}000 \times g$ at 4 °C for 10 min and pellets are rejected in order to clean the CSF of unwanted insoluble particles or cell debris. The supernatants are then maintained at -80 °C until used. The study by Sakai et al. (4), in which the authors isolated CA from brain tissue, indicated that centrifugation at $650 \times g$ during 10 min is enough to produce CA precipitation. Therefore, as the standard protocol used by the Biobanc would remove any CA present in the CSF, we asked for samples of noncentrifuged CSF in order to perform a prospective study. These CSF samples were extended on slides and were stained with periodic acid Schiff (PAS) or immunostained with human IgMs directed against the neoepitopes (IgM$_h$ α-NE). In all cases, we observed round bodies with sizes and histochemical staining compatible with CA, thus suggesting the presence of CA in the CSF. Representative images of these bodies stained with PAS or with IgM$_h$ α-NE are shown in Fig. 3 *A* and *B*, respectively. As the use of noncentrifuged samples compromises the availability of CSF for other studies, the Biobanc began to collect the pellets of the CSF processed according to their protocol instead of rejecting them. These pellets were used to complete the present study. When performing the extensions from resuspended pellets of CSF, CA were also observed stained with PAS (Fig. 3*C*) and stained with both α-GS and IgM$_h$ α-NE (Fig. 3*D*). The presence of CA in pellets of CSF was corroborated by visualizing them at an ultrastructural level using transmission electron microscopy (TEM). As shown by the representative images from Fig. 3 *E–J*, CA from CSF comprise densely packed, randomly oriented short linear fibers, which in some cases are concentrated in the central region or in concentric ring regions of CA. Indeed, these ultrastructural features are similar to those of mature CA from the hippocampus brain tissue (8) and those of mature PAS granules from mice (30), which are equivalent to CA of human brain. CA from the brain are encircled by a plasma membrane that confirms their intracellular and cytosolic location (3, 8), but this membrane is not visible in CA from the CSF. This suggests that CA may have lost this membrane during the extrusion process. Sbarbati et al. (7) also suggested this hypothesis when describing the extrusion of CA to pial connective tissue from vestibular nerve samples. Scanning electron microscope
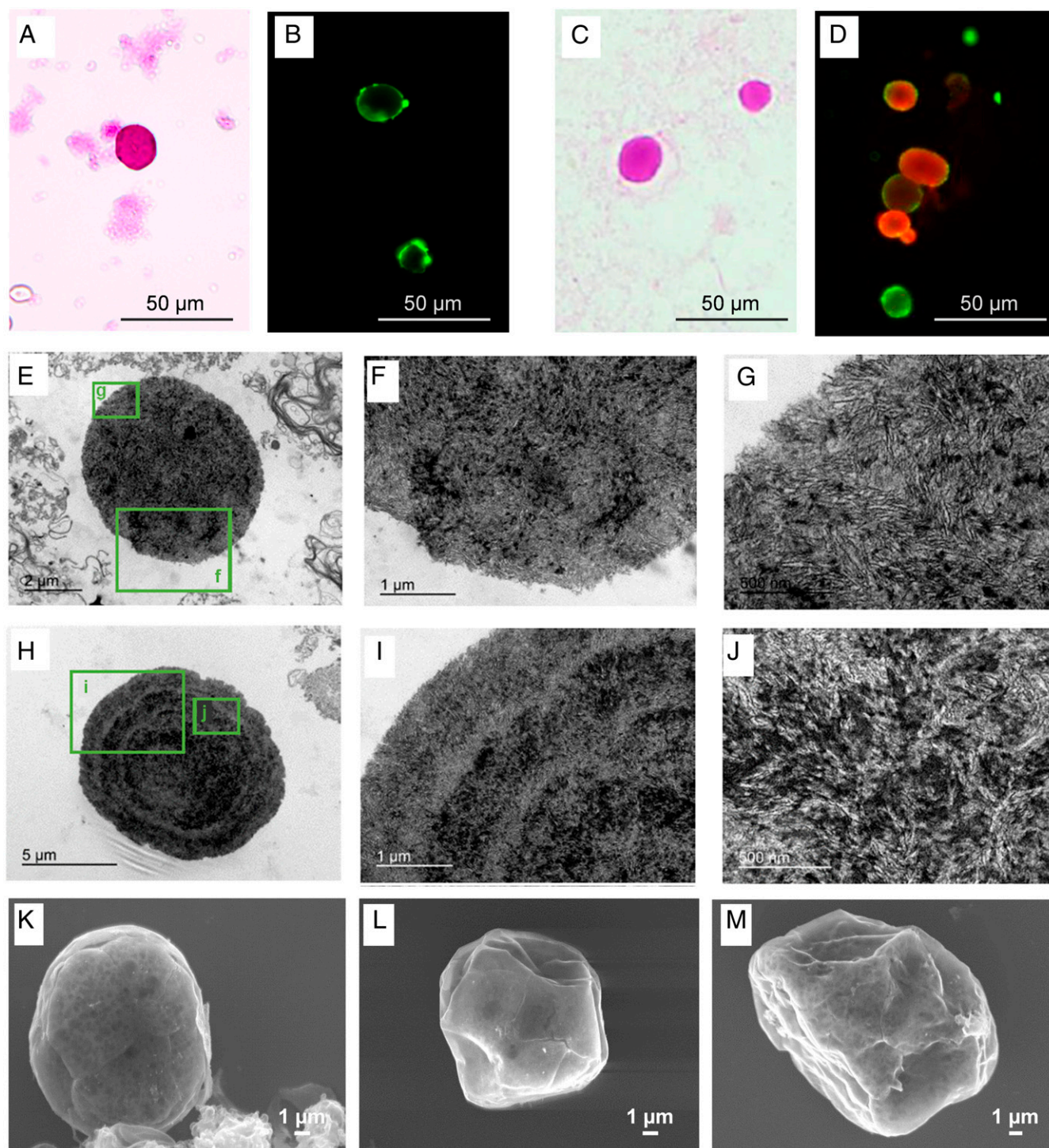
Fig. 3. Human CSF contains CA. After the extension of uncentrifuged CSF on slides, the staining with PAS (*A*) and with IgM$_h$ α-NE (*B*) showed the presence of CA in CSF. When performing the extension from resuspended pellets of CSF, CA were also observed stained with PAS (*C*) and stained with both α-GS and IgM$_h$ α-NE (*D*, red and green, respectively). This indicated that pellets of CSF contain CA. The presence of CA in pellets of CSF is corroborated by visualizing them at an ultrastructural level using TEM (*E–J*) and SEM (*K–M*).

(SEM) analysis from pellet samples also confirmed the presence of CA in CSF (Fig. 3 *K–M*). As reported many years ago with reference to CA isolated from brain tissue (4), these bodies present a spherical shape with a smooth surface. Ripples and crevices may be observed on the surface, but these are artifacts produced by the electron beam interacting on the sample. Altogether, these results indicate that CSF contains CA, thus demonstrating that CA are

extruded from brain to the CSF. Moreover, these results also indicate that CSF pellets can be used to analyze these bodies.

CA Are Present in the Cervical Lymph Nodes. Once the presence of CA in the CSF is established, the next question is to determine whether they are eliminated from the CSF. Due to their size (some 10 μm in diameter) they cannot be eliminated via arachnoid

granulations to dural venous sinuses. However, as noted above, CSF and their macromolecules are also drained via the meningeal lymphatic system, and thus CA may be eliminated by this system and may then be driven to the cervical lymph nodes.

We therefore analyzed cervical lymph nodes from different cases in order to check the presence of CA. When staining paraffin-embedded sections of the cervical nodes with PAS we observed that, although not all sections contain CA, these bodies were observed in certain sections from all donors (Fig. 4). As can be seen in Fig. 4A, CA found in the cervical lymph nodes were generally sited in the subcapsular space or in the trabecular sinuses that radiate from this space through the parenchyma to the medullary sinuses. It can also be seen that, although CA are surrounded by the sinus space, they are not completely free; they show specific contacts with some lymph node cells. The localization of these lymph node cells in the trabecular sinuses and their elongated form suggest that they can be macrophages entrapping CA. We also analyzed different sections by immunofluorescence techniques. The staining with IgM_h α-NE and the secondary fluorochrome-labeled α-IgM_h antibody did not allow the visualization of CA in the nodes because of the presence of IgM_h in the tissue, which become fluorolabeled and thus masked CA visualization. However, CA were observed in the nodes when using IgMs from mouse directed against neoepitopes (IgM_m α-NE) and a secondary fluorochrome-labeled α-IgM_m (Fig. 4B). As shown in previous research (6), the α-IgM_m binds to the IgM_m but does not recognize the IgM_h. In order to determine what type of lymph node cells were in contact with CA, we used double immunostaining with IgM_m α-NE and α-FcμR on the one hand and IgM_m α-NE and α-CD35 on the other. The FcμR (or FAIM3) is an IgM receptor present in some macrophages and dendritic cells and is related to phagocytic processes, and CD35 is a receptor for the C3b component of the complement system also present in these cells. We observed that cervical lymph nodes contain some cells that become stained with these markers, but the cells that are in contact with CA did not stain with these antibodies (Fig. 4C).

We also analyzed the relationship between the amount of CA contained in the cervical nodes and the position of these nodes in the neck, expecting that nodes sited in the lower regions would have fewer CA than those in the upper regions. We analyzed the amount of CA in the nodes sited in regions I, II, III, and IV according to Rouvière's standard anatomic description (31). Regions I and II are located in the upper plane of the neck, while region III is located in the intermediate plane and region IV in the lower plane. Data on these observations can be found in the [Dataset S1](#). Fig. 4C shows the mean number of CA per section according to the localization of the node in the neck. The mean number of CA $\pm$ SEM from sections corresponding to the upper zone (regions I and II) is 1.62 ± 0.31 ($n = 13$), from the intermediate zone (region III) 0.90 ± 0.31 ($n = 10$), and from the lower zone (region IV) 0.17 ± 0.17 ($n = 6$) (Fig. 4D). These results correspond to the mean of CA per section. Bearing in mind that each section has a thickness of 8 μm, and considering that the standard size of a node is around 3 mm in radius, the approximate mean number of CA per node is about 810 ± 155.45 in the upper zone, 450 ± 157.17 in the intermediate zone, and 85 ± 83.28 in the lower zone. Then, an ANOVA was performed with the number of CA per section as the dependent variable and the zone where the nodes are located as the independent variable. The ANOVA indicated significant differences in the number of CA according to zone ($F_{2.26} = 4.74$; $P < 0.019$). Post hoc comparisons (Bonferroni test) indicated higher numbers of CA in the nodes of the upper zone than in those of the lower zone ($P < 0.017$). There were no significant differences in the number of CA in the nodes of the intermediate zone compared with the upper and lower zones ($P > 0.05$). Overall, these results support the idea that CA reach and become entrapped in the cervical lymph nodes.

Macrophages Phagocytose and Process CA. As indicated above, CA in cervical lymph nodes were generally found in the subcapsular space or in the trabecular sinuses and have specific contacts with some lymph node cells. Although α-CD35 and α-FcμR do not seem to stain these lymph node cells, the localization of these cells in the trabecular sinuses and their elongated form suggest that they may be macrophages entrapping CA.

Subsequently, we used in vitro cultures of macrophages derived from THP-1 cells to analyze their interaction with CA. In the first attempt, we isolated CA from CSF and opsonized them with IgM_h α-NE, and then added the opsonized CA in the culture of THP-1–derived macrophages. PAS staining applied to these samples suggested that macrophages can phagocytose CA. As illustrated in Fig. 5A, some macrophages are close to CA and begin to encircle them, while in other cases macrophages completely encircle CA, suggesting that the CA have been phagocytosed. When staining the samples with fluorescent-labeled phalloidin and fluorescent-labeled α-IgM_h we also observed some CA adhering to the macrophages and others encircled by them (Fig. 5B). Using confocal microscopy and 3D reconstruction, which allow observing the structure rotating on itself, we observed some macrophages that were phagocytosing CA (Fig. 5C) and also some others containing CA inside them, indicating that the CA had been phagocytosed (Fig. 5D). Other samples were processed for visualization by SEM. SEM images also showed macrophages engulfing CA, and some filopodia were seen emerging from macrophages and coming into contact with the bodies (Fig. 5E). Altogether, these results indicate that CA opsonized with IgM_h can be phagocytosed by THP-1–derived macrophages.

Unexpectedly, however, controls performed with CA non-opsonized with IgMs were also phagocytosed by THP-1–derived macrophages (Fig. 5F). Therefore, although the possibility that opsonization with IgMs could generate some response cannot be ruled out, IgM opsonization is not a requisite for CA phagocytosis by THP-1–derived macrophages, and this process must involve other mechanisms than those triggered by IgMs and α-FcμR. Phagocytosis via the IgM activation of the complement system (32) can also be ruled out because in our experiments the complement proteins were heat inactivated. Mei Liu et al. (33) observed that CA are reactive for Con A, a lectin that binds with high affinity to mannose oligomers, and indicated that CA contain mannose-rich conjugates. Thus, as mannose conjugates can be recognized by mannose receptors sited in macrophages and can activate phagocytosis, it may be that mannose contained on the surface of CA can trigger phagocytosis via possible mannose receptors sited on THP-1–derived macrophages. Accordingly, we first verified that CA are reactive to Con A. Fig. 5G shows representative images of CA from CSF stained with Con A, which suggests the presence of mannose in CA. We then tested the presence of the mannose receptor CD206 in THP-1–derived macrophages, and observed that actually macrophages became stained with α-CD206, indicating the presence of this receptor in these cells. Fig. 5H shows a representative image of a CA (stained with fluorescent-labeled Con A) encircled by THP-1 macrophages immunostained with α-CD206. These results reinforce the notion that, in the case of THP-1 cells and with the conditions of the present study, the phagocytosis of CA is produced via the mannose receptor. However, as will be discussed below, there may be other redundant mechanisms by which macrophages can phagocytose CA.

Discussion

For decades now, several functions have been attributed to CA, all of them proposed on the basis of studies performed in brain tissue or its extracts. The presence of CA in both the CSF and the cervical lymph nodes, demonstrated in the present study, provides another perspective.
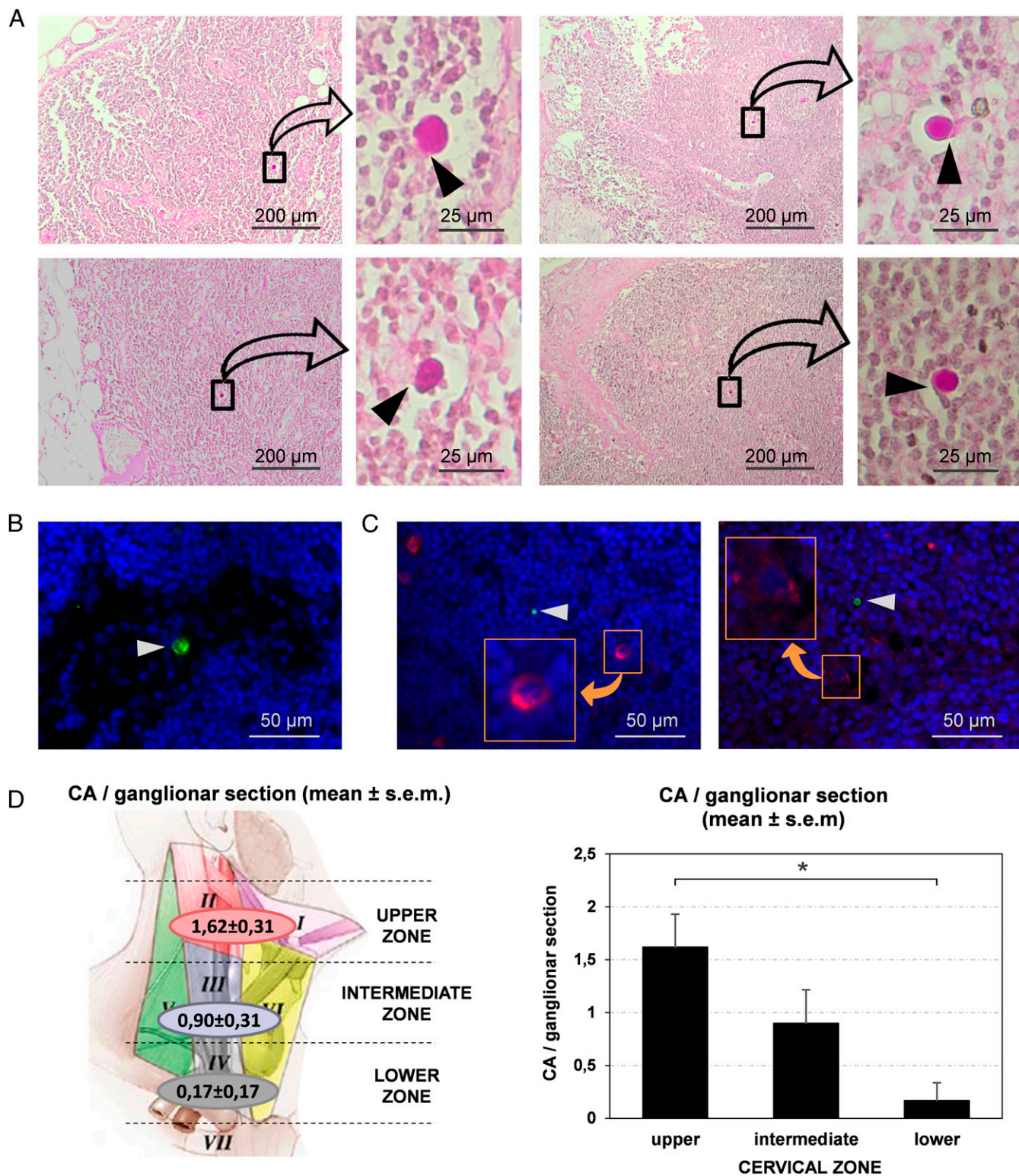
Riba et al.

Fig. 4. CA are present in the cervical lymph nodes. (A) Images of sections from different cervical nodes stained with PAS. For each section, a region containing CA is magnified. Note that CA exhibit specific contacts with some lymph node cells (arrowheads). (B) CA (arrowhead) can also be observed by immunofluorescence when sections are immunostained by IgM_m α-NE (green). Blue staining (Hoechst) corresponds to the nuclei of lymph node cells. (C) Double staining with IgM_m α-NE and α-FcμR (green and red respectively, *Left* image), and double staining with IgM_m α-NE and α-CD35 (green and red respectively, *Right* image) indicate that some cells of the cervical lymph nodes contain FcμR and other cells express CD35 (*Insets*). However, the cells in contact with CA (arrowheads) did not stain with these antibodies. (D) Mean number (±SEM) of CA per section in the different regions of the neck. The upper region of the neck contains more CA per section than the lower one ($P < 0.05$), which suggests that brain CA reach the cervical lymph nodes, and that the nodes may retain or eliminate them.
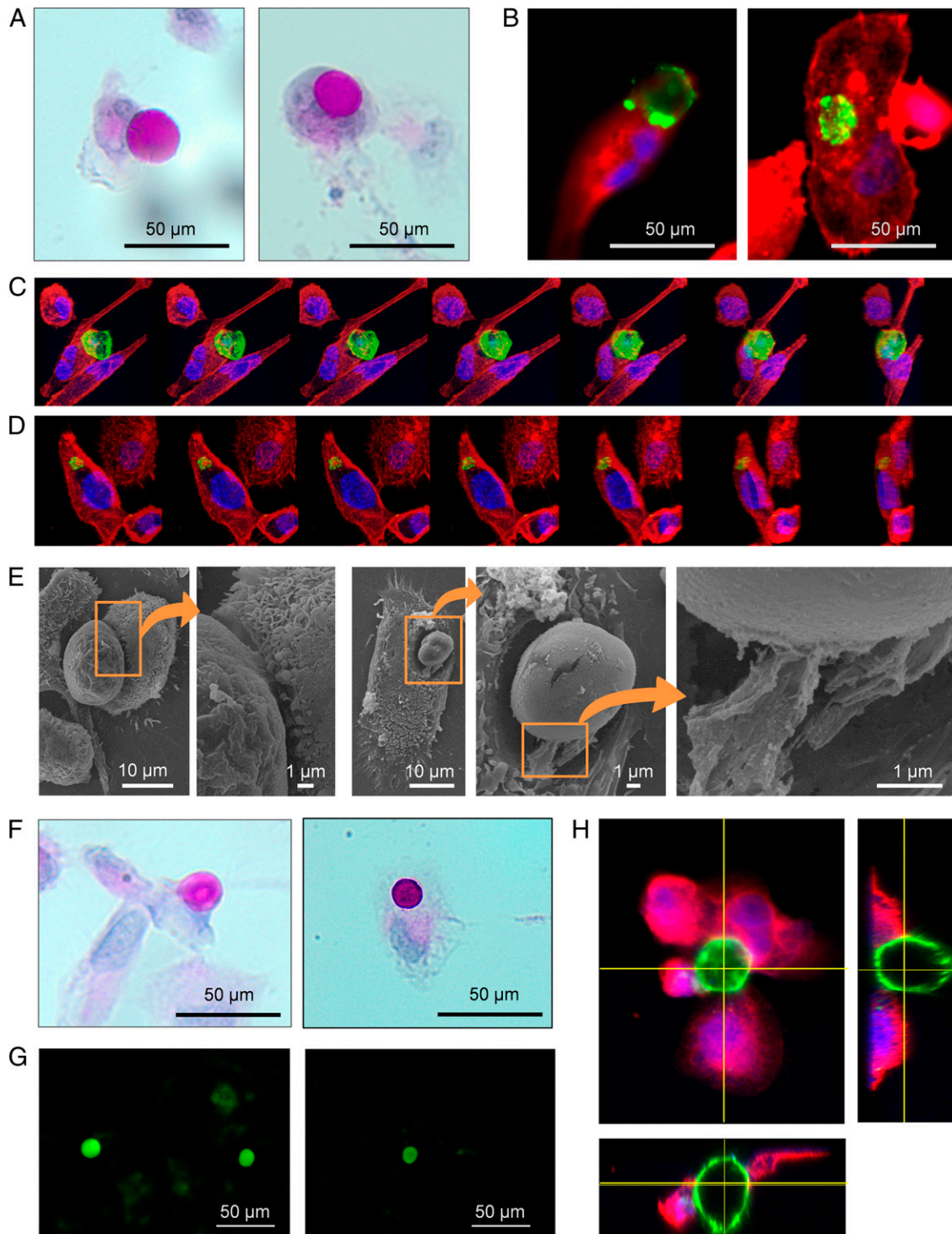
Riba et al.

PHYSIOLOGY

Fig. 5. CA are phagocytosed by THP-1–derived macrophages. (*A*) Macrophage in contact with an IgM$_h$-opsonized CA (*Left*) and an IgM$_h$-opsonized CA phagocytosed by macrophage (*Right*); PAS staining. (*B*) Other examples of a macrophage making contact with an IgM$_h$-opsonized CA (*Left*) and an IgM$_h$-opsonized CA phagocytosed by macrophage (*Right*). In these cases, macrophages are stained with fluorescent-labeled phalloidin (red) and IgM$_h$-opsonized CA are stained with fluorescent-labeled α-IgM$_h$ (green). Nuclei are stained with Hoechst (blue). (*C*) Sequence of images showing a macrophage phagocytosing an IgM$_h$-opsonized CA from different points of view. The sequence was performed after the 3D reconstruction from images obtained by confocal microscopy. Phalloidin (red), fluorescent labeled α-IgM$_h$ (green), and Hoechst (blue). (*D*) The same procedure was used to obtain a sequence of images showing an IgM$_h$-opsonized CA that has been phagocytosed by a macrophage. (*E*) SEM images also showed macrophages engulfing IgM$_h$-opsonized CA. Some filopodia were found emerging from macrophages and making contact with the bodies (*Insets*). (*F*) Macrophage making contact with a non IgM$_h$-opsonized CA (*Left*) and a non IgM$_h$-opsonized CA phagocytosed by a macrophage (*Right*); PAS staining. These results indicate that IgM$_h$ opsonization of CA is not a requirement for phagocytosis by THP-1–derived macrophages. (*G*) CA from CSF become stained with fluorochrome-labeled Con A, which suggests that they contain mannose. (*H*) CA (stained with Con A, green), encircled by THP-1–derived macrophages immunostained with α-CD206 (mannose receptor, red) and Hoechst (nuclei, blue). Orthogonal views show macrophages attached to the CA. These results suggest that, in the case of THP-1–derived macrophages and with the conditions set up in the present study, CA phagocytosis is produced via the mannose receptor.

CA are formed by waste elements included in a polyglucosan structure and their presence in the CSF reveals that they may act as waste containers removing brain products from the brain to the CSF. In addition, their presence in the deep cervical lymph nodes supports the hypothesis that they can leave CSF via the meningeal lymphatic vessels and reach these nodes. As shown, the staining properties of the CA found in the cervical nodes indicate that they are compatible with those described in the CSF, and their localization in the trabecular sinuses but not in the parenchyma suggests that they are not generated in the nodes themselves. In addition, the gradient in the number of CA observed in the nodes related to their proximity to the brain also suggests that they arrive there from the CSF. As there are other structures apart from the brain that generate CA, the possibility that the CA contained in the cervical nodes come from some of these other structures must be considered. If this were the case, then: 1) these structures must generate CA that become stained with PAS and immunostained with natural IgMs; 2) these structures must expel the CA directly or indirectly into the lymph; and 3) the lymph generated must drain toward the cervical lymph nodes sited in the regions I, II, III, and IV of the neck. To our knowledge, the brain is the only structure that fulfills the 3 premises indicated. Structures or organs like mammary glands, cardiac muscle, or prostate can be ruled out, because the lymph of these structures does not drain toward the cervical lymph nodes. On the other hand, CA originating in the thyroid gland and prostate are calcified structures formed (in the case of prostate) by a calcified protein matrix (34), and thus are incompatible with the CA that we described in the cervical lymph nodes. This is also the case of calculi originating in the salivary gland, which are formed by hydroxyapatite (34).

Although it might be thought that the presence of CA in the CSF is merely circumstantial, there are certain indices that suggest that this presence is the result of some specific physiological processes. The localization of CA mainly in the periventricular and subpial regions of the brain does not seem to be casual. Moreover, as can be observed in Movie S1 (adapted from ref. 5), some CA contain a central compact core with a high presence of ubiquitin and a peripheral region which contains GS, p62, and ubiquitin. The central core may correspond to a region where different ubiquitinated waste substances have accumulated, while the peripheral region may correspond to an active zone where the waste elements are collected by p62 and packaged by GS, which generates the polyglucosan component of the CA (5). In addition, the presence in CA of neoepitopes that are recognized by plasmatic natural IgMs suggested that they may be structures ready to be phagocytosed by macrophages or other immune cells if they were released from the brain (6, 8). Correspondingly, and as shown here, the CA present in the cervical lymph nodes were seen adhered to elongated cells compatible with macrophages, and CA were avidly phagocytosed by THP-1–derived macrophages. Taken together, these results extend the hypothesis proposed in Augé et al. (6), according to which CA collect residual substances and are removed from the brain and then eliminated via the immune system. Fig. 6 summarizes this route, updating the scheme proposed in 2017. The pathway begins in the astrocytes which generate CA to create a kind of waste container formed by polyglucosan aggregates that amass waste products originating not only in the astrocytes themselves, but also deriving from neighboring cells. Aging and neurodegenerative conditions increase the production of waste products, thus enhancing the process. After their release into the CSF, CA reach the cervical lymph nodes via the meningeal lymphatic vessels and the subsequent lymphatic vessels. There, mannose contained in CA can trigger the phagocytosis via mannose receptors sited on macrophages, although we do not rule out other possible mechanisms including the IgM-FcμR, the IgM-complement pathways, and the lectin pathway mediated by the C3b opsonization induced by mannose-binding

lectin (MBL). In any case, the immune system may provide redundant mechanisms to ensure the elimination of CA.

Due to the blood–brain barrier and the cerebrospinal fluid–brain barrier, the brain used to be considered an immune-privileged organ until the discovery of the meningeal lymphatic system. This system collects brain substances contained in the CSF, and the presence of specific brain components outside the brain can interact with the immune system with possibly fatal consequences (35, 36). It has been reported that cellular and soluble constituents of the CSF cause immune responses in the cervical lymph nodes (18), and the possible immunological implications of CSF drainage via the meningeal lymphatic system were also noted long ago by Bradbury et al. (37). In this regard, Weller et al. (21) indicated that "the lymphatic drainage of ISF and CSF and the specialized cervical lymph nodes to which they drain play significant roles in the induction of immunological tolerance and of adaptive immunological responses in the central nervous system (CNS)". Accordingly, and given that the results of the present study indicate that CA reach the cervical lymph nodes, we cannot rule out the possibility that, in certain circumstances, the waste substances contained in CA may enhance certain immunological functions or intervene in some autoimmune alterations. Consequently, and given their possible clinical implications, the possible role of CA in immunological processes or brain autoimmune diseases needs to be investigated.

Our findings may also represent a starting point for the study of some clinical markers of brain disorders. We know that CA can contain waste substances produced in the brain and several of them may be markers of some of these disorders. We also know that CA are present in both noncentrifuged samples of CSF and pellets obtained from CSF centrifugation, and so these structures are easily accessible for study. In recent decades, the liquid fraction of the CSF has been exhaustively assessed in order to obtain brain markers. For instance, it is well established that phospho-tau181, total-tau, and amyloid β1–42 are CSF biomarkers for Alzheimer's disease (38). Moreover, promising new fluid biomarkers for staging and monitoring of frontotemporal dementia, such as the neurofilament light chain, are emerging (39, 40). Furthermore, CSF analysis is used to exclude other diseases in the differential diagnosis of multiple sclerosis (41). In addition, CSF biomarkers are being studied in patients with Parkinson's and are being used in clinical trials (42). However, the solid fraction of the CSF has not been studied to obtain brain markers. Our results support the need to study CA contained in the CSF, postulating that these bodies will contain some of these markers. As CA from CSF are more accessible than those from brain tissue, their use for diagnostic purposes may become a valuable new strategy.

To sum up, our results indicate that CA can act as waste containers that allow the removal of waste products from the brain and suggest their involvement in a mechanism that cleans the brain. Moreover, we hypothesize a role for CA in some autoimmune brain diseases, exporting brain substances that interact with the immune system, and we suggest that they may be important elements in the diagnosis of certain brain diseases, since they may contain markers of brain disease.

Methods

Human CSF Samples. Postmortem CSF samples from 16 cases of neuropathologically affected patients (65 to 90 y old) were obtained from the Banc de Teixits Neurològics (Biobanc-Hospital Clínic-IDIBAPS, Barcelona). Noncentrifuged samples ($n = 7$) as well as pellets obtained after centrifugation at $4,000 \times g$ at 4 °C for 10 min ($n = 9$) were used. Medical data on these cases are detailed in SI Appendix, Table S1.

Human Deep Cervical Lymph Node Samples. Paraffin sections (thickness of 8 μm) of cervical lymph nodes taken by lymphadenectomy from 4 cancer patients (83 to 96 y old) were obtained from the Banc de Tumors i Anatomia Patològica (Biobanc-Hospital Clínic-IDIBAPS, Barcelona). All selected nodes

PHYSIOLOGY

Fig. 6. Hypothesized pathway of the elimination of brain waste products based on the role of CA as waste containers. The pathway begins in the astrocytes, which generate CA building a kind of waste container formed by polyglucosan aggregates that amass waste products originated not only in the astrocytes themselves, but also derived from neighboring cells (*1*). CA are then released into the CSF in the ventricular region or subarachnoid space (*2a* and *2b*) or via the glymphatic system (*2c*). From there (*3*), CA enter the meningeal lymphatic vessels (*4*) and the subsequent lymphatic vessels (*5*) and reach the cervical lymph nodes (*6*). There, macrophages can phagocyte CA via mannose and mannose receptors or via other possible mechanisms that might include the IgM-FcμR, the IgM-complement pathways, and the lectin pathway mediated by the C3b opsonization induced by MBL and C3b receptors (*7*). C3, C3 component of the complement system; C3b, C3b fragment generated from C3; CR, C3b receptor; ManR, mannose receptor; UPS, ubiquitin–proteasome system. (See text for details.)

were nontumor affected. Medical data on these cases are detailed in *SI Appendix*, Table S2.

All procedures involving human samples were performed in accordance with appropriate guidelines and regulations. All experiments involving human tissue were approved by the Bioethical Committee of the University of Barcelona.

Cell Culture and Differentiation. THP-1 cells provided by ATCC were cultured as previously described (43). Cells were subcultured at a density of 5×10^4 cells/cm^2 on 24-well clusters with 12-mm round cover glasses. Cells were differentiated to macrophages with phorbol 12-myristate 13-acetate (PMA; Sigma-Aldrich) at a concentration of 100 nmol/L in RPMI 1640 (Sigma-Aldrich) supplemented with 10% heat-inactivated FBS (GE Healthcare Life Sciences), 50 μM β-mercaptoethanol (Sigma-Aldrich), and penicillin (100 U/mL)/streptomycin (100 μg/mL) (Life Technologies) for 3 d. Differentiation of PMA-treated cells was enhanced after the initial 3-d stimulus by removing the PMA-containing media and then incubating the cells in fresh supplemented RPMI 1640 for a further 3 d.

Phagocytosis Studies. To study the phagocytosis of CA by macrophages, we first obtained CA from CSF and opsonized them with IgMs. CA were obtained from CSF samples completing 5 centrifugations of CSF at $700 \times g$ for 10 min, discarding the supernatants, and resuspending the pellets with 500 μL of PBS. Thereafter, another centrifugation at $700 \times g$ for 10 min was performed, but the resuspension was obtained with 500 μL of PBS containing IgM$_h$ (1:10 dilution; OBT1524; AbD Serotec). The resuspension was maintained overnight at 4 °C to obtain the IgM-opsonized CA. Controls were performed with PBS without IgMs. Thereafter, another centrifugation at $700 \times g$ for 10 min was performed, and the pellet was resuspended with 1,000 μL of supplemented RPMI. The samples of 1,000 μL were then added to the wells containing the THP-1–derived macrophages after removing their media.

Antibodies and Reagents. The following antibodies were used as primary antibodies: human IgM purified immunoglobulins (1:10 dilution; OBT1524; AbD Serotec), rabbit monoclonal IgG against GS (1:100; 15B1; Cell Signaling), IgMs contained as a contaminant in the OX52 antibody (obtained from mouse

ascites), rabbit polyclonal IgG against mannose receptor CD206 (1:1,200; ab64693, Abcam), mouse monoclonal IgG$_1$ against CD35 (1:40; E11; Thermo Scientific), and mouse monoclonal IgG$_1$ against FcμR (1:150; OTI1E6; Thermo Scientific).

The following antibodies were used as secondary antibodies: Alexa Fluor (AF) 488 goat anti-human IgM heavy chain (1:200; A-21215; Life Technologies), AF488 goat anti-mouse IgM μ chain specific (1:250; 115-545-075; Jackson ImmunoResearch Laboratories), AF555 donkey anti-rabbit IgG directed against both heavy and light chains (1:250; A-31572; Life Technologies), and AF555 goat anti-mouse IgG$_1$ (1:250; A-21125; Life Technologies).

Fluorescein-labeled Con A (Vector Laboratories) was incubated overnight instead of primary antibodies in some immunohistochemical experiments in order to detect CA.

Tetramethyl rhodamine-isothiocyanate (TRITC)-phalloidin (Sigma-Aldrich) was used to stain F-actin from macrophages. This staining was combined with the immunohistochemical procedures and was performed by adding TRITC-phalloidin (1:500) to the secondary antibodies.

Immunofluorescence. Volumes of 40 μL of noncentrifuged CSF or 40 μL of resuspended CSF pellets (centrifuged 6 times at 700 × g for 10 min and resuspended each time with PBS) were extended in slides and air dried. They were then fixed with acetone for 10 min at 4 °C to carry out the immunohistochemistry. For lymph node samples, sections were deparaffinized in xylene and an antigen retrieval step was applied with 10 mM sodium citrate buffer (pH = 6.0) heated to 100 °C for 40 min. For the cell culture, macrophages were washed with Dulbecco's PBS (DPBS; GIBCO) and fixed in 4% paraformaldehyde in PBS for 15 min.

Immunofluorescence was performed as follows: samples were rehydrated with PBS and then blocked and permeabilized with 1% BSA in PBS (Sigma-Aldrich) (blocking buffer [BB]) with 0.1% Triton X-100 (Sigma-Aldrich) for 20 min. They were then washed with PBS and incubated with the primary antibody overnight at 4 °C. Next, samples were washed and incubated for 1 h at room temperature with the secondary antibody. Nuclear staining was performed with Hoechst (2 μg/mL, H-33258, Fluka) and samples were washed and coverslipped with Fluoromount (Electron Microscopy Sciences) or ProLong Gold (Thermo Scientific). Staining controls were performed by incubating with BB instead of the primary antibody. In double staining, controls for cross-reactivity of the antibodies were also performed.

PAS Staining. All samples were processed as described in the immunohistochemistry section, except for the macrophage cell culture, in which cells were only washed with DPBS. Then, samples were stained with PAS according to the standard procedure. Briefly, samples were fixed for 10 min in Carnoy's solution (60% ethanol, 30% chloroform, and 10% glacial acetic acid). Thereafter, the samples were pretreated for 10 min with 0.25% periodic acid (19324-50, Electron Microscopy Sciences) in distilled water followed by a washing step for 3 min. Then, the samples were immersed in Schiff's reagent (26052-06, Electron Microscopy Sciences) for 10 min. After Schiff's reagent, samples were washed for 5 min in distilled water. Nuclei were counterstained for 6 min with a hematoxylin solution according to Mayer (3870, J. T. Baker). Then, the samples were washed, dehydrated to xylene, and coverslipped with a quick mounting medium (Eukitt, Fluka Analytical).

Sample Processing for Transmission Electron Microscopy. CSF samples were postfixed for 1 h using 4% paraformaldehyde and 0.1% glutaraldehyde in phosphate buffer (PB) 0.1 M. Next, samples were centrifuged at 700 × g for 10

min and washed 4 times with PB 0.1 M for 10 min. Then, they were stained with 1% OsO4 in PB and containing 0.8% potassium ferricyanide for 1 h at 4 °C, dehydrated in acetone at 4 °C, and finally embedded in Spurr resin. The resin was polymerized for 48 h at 80 °C. Semithin sections (1-μm thickness) were obtained and, after methylene blue staining, CA were localized. Ultrathin sections (70-nm thickness) were obtained using an ultramicrotome (Leica Ultracut) and a diamond knife (Diatome), and the sections were then placed on copper grids and poststained with uranyl acetate and lead citrate.

Sample Processing for Scanning Electron Microscopy. CSF samples and macrophages were postfixed using 2.5% glutaraldehyde in PB 0.1 M. Next, they were washed 3 times with PB 0.1 M for 10 min. Then, samples were stained with 1% OsO4 in PB and containing 0.8% potassium ferricyanide for 1 h 30 min at 4 °C and dehydrated in alcohols at 4 °C. Next, they were processed either via critical point drying or air drying with hexamethyldisilazane. Finally, they were mounted and sputter coated (carbon or gold).

Image Acquisition and Processing. Images were captured with a fluorescence laser in an optical microscope (BX41, Olympus) and stored in TIFF format. All of the images were acquired using the same microscope, laser, and software settings. Exposure time was adapted to each staining, but the respective control images were acquired with the same exposure time. Image analysis and treatment were performed using the ImageJ program (NIH). Images that were modified for contrast and brightness to enhance their visualization were processed in the same way as the images corresponding to their respective controls.

In order to study the CA on cell cultures, image stacks were taken with a confocal laser scanning microscope (LSM 880, Zeiss) and 3D animations were obtained by means of the ImageJ program (NIH).

Ultrathin sections were examined using a JEOL JEM-1010 transmission electron microscope operated at an accelerating voltage of 80 kV. The images were obtained using a CCD Orius camera (Gatan).

SEM images were observed using a JEOL JSM-7001F scanning electron microscope.

Statistical Analysis. Statistical analysis was performed with the ANOVA module of the IBM SPSS Statistics (IBM). Significant differences were considered when $P < 0.05$.

Data Availability Statement. All data are available in the manuscript and supporting information.

1. G. Catola, N. Achúcarro, Über die Enstehung de Amyloidkörperchen in Zentralnervensystem. *Virchows Arch. f. Path. Anat.* **184**, 454–469 (1906).
2. R. Virchow, Ueber eine Gehirn und Ruckenmark des Menschen aufgefundene Substanz mit der chemischen Reaction der Cellulose. *Arch. Pathol. Anat. Physiol. Klin. Med.* **6**, 135–138 (1854).
3. J. B. Cavanagh, Corpora-amylacea and the family of polyglucosan diseases. *Brain Res. Brain Res. Rev.* **29**, 265–295 (1999).
4. M. Sakai, J. Austin, F. Witmer, L. Trueb, Studies of corpora amylacea. I. Isolation and preliminary characterization by chemical and histochemical techniques. *Arch. Neurol.* **21**, 526–544 (1969).
5. E. Augé, J. Duran, J. J. Guinovart, C. Pelegrí, J. Vilaplana, Exploring the elusive composition of corpora amylacea of human brain. *Sci. Rep.* **8**, 13525 (2018).
6. E. Augé, I. Cabezón, C. Pelegrí, J. Vilaplana, New perspectives on corpora amylacea in the human brain. *Sci. Rep.* **7**, 41807 (2017).
7. A. Sbarbati, M. Carner, V. Colletti, F. Osculati, Extrusion of corpora amylacea from the marginal glia at the vestibular root entry zone. *J. Neuropathol. Exp. Neurol.* **55**, 196–201 (1996).
8. E. Augé et al., Corpora amylacea in human hippocampal brain tissue are intracellular bodies that exhibit a homogeneous distribution of neo-epitopes. *Sci. Rep.* **9**, 2063 (2019).
9. S. Cissé, H. M. Schipper, Experimental induction of corpora amylacea-like inclusions in rat astroglia. *Neuropathol. Appl. Neurobiol.* **21**, 423–431 (1995).
10. H. M. Schipper, S. Cissé, Mitochondrial constituents of corpora amylacea and autofluorescent astrocytic inclusions in senescent human brain. *Glia* **14**, 55–64 (1995).
11. K. Selmaj et al., Corpora amylacea from multiple sclerosis brain tissue consists of aggregated neuronal cells. *Acta Biochim. Pol.* **55**, 43–49 (2008).
12. S. Cissé, G. Lacoste-Royal, J. Laperrière, T. Cabana, D. Gauvreau, Ubiquitin is a component of polypeptides purified from corpora amylacea of aged human brain. *Neurochem. Res.* **16**, 429–433 (1991).
13. N. A. Jessen, A. S. Munk, I. Lundgaard, M. Nedergaard, The glymphatic system: A beginner's guide. *Neurochem. Res.* **40**, 2583–2599 (2015).
14. D. Pirici, C. Margaritescu, Corpora amylacea in aging brain and age-related brain disorders. *J. Aging Gerontol.* **2**, 33–57 (2014).
15. F. Bucchieri, F. Farina, G. Zummo, F. Cappello, Lymphatic vessels of the dura mater: A new discovery? *J. Anat.* **227**, 702–703 (2015).
16. M. Földi et al., New contributions to the anatomical connections of the brain and the lymphatic system. *Acta Anat. (Basel)* **64**, 498–505 (1966).

PHYSIOLOGY

17. M. Johnston, A. Zakharov, C. Papaiconomou, G. Salmasi, D. Armstrong, Evidence of connections between cerebrospinal fluid and nasal lymphatic vessels in humans, non-human primates and other mammalian species. *Cerebrospinal Fluid Res.* **1**, 2 (2004).

18. A. Louveau *et al.*, Structural and functional features of central nervous system lymphatic vessels. *Nature* **523**, 337–341 (2015).

19. A. Louveau *et al.*, Understanding the functions and relationships of the glymphatic system and meningeal lymphatics. *J. Clin. Invest.* **127**, 3210–3219 (2017).

20. S. K. Ha, G. Nair, M. Absinta, N. J. Luciano, D. S. Reich, Magnetic resonance imaging and histopathological visualization of human dural lymphatic vessels. *Bio Protoc.* **8**, 1–17 (2018).

21. R. O. Weller, I. Galea, R. O. Carare, A. Minagar, Pathophysiology of the lymphatic drainage of the central nervous system: Implications for pathogenesis and therapy of multiple sclerosis. *Pathophysiology* **17**, 295–306 (2010).

22. M. D. Sweeney, B. V. Zlokovic, A lymphatic waste-disposal system implicated in Alzheimer's disease. *Nature* **560**, 172–174 (2018).

23. L. Sakka, G. Coll, J. Chazal, Anatomy and physiology of cerebrospinal fluid. *Eur. Ann. Otorhinolaryngol. Head Neck Dis.* **128**, 309–316 (2011).

24. C. Grönwall, J. Vas, G. J. Silverman, Protective roles of natural IgM antibodies. *Front. Immunol.* **3**, 66 (2012).

25. S. Brändlein *et al.*, Natural IgM antibodies and immunosurveillance mechanisms against epithelial cancer cells in humans. *Cancer Res.* **63**, 7995–8005 (2003).

26. H. P. Vollmers, S. Brändlein, Natural IgM antibodies: The orphaned molecules in immune surveillance. *Adv. Drug Deliv. Rev.* **58**, 755–765 (2006).

27. A. Goldin, J. A. Beckman, A. M. Schmidt, M. A. Creager, Advanced glycation end products: Sparking the development of diabetic vascular injury. *Circulation* **114**, 597–605 (2006).

28. B. A. Cobb, D. L. Kasper, Coming of age: Carbohydrates and immunity. *Eur. J. Immunol.* **35**, 352–356 (2005).

29. A. Suzuki *et al.*, Phagocytized corpora amylacea as a histological hallmark of astrocytic injury in neuromyelitis optica. *Neuropathology* **32**, 587–594 (2012).

30. G. Manich *et al.*, Presence of a neo-epitope and absence of amyloid beta and tau protein in degenerative hippocampal granules of aged mice. *Age (Dordr.)* **36**, 151–165 (2014).

31. H. Rouvière, A. Delmas, *Anatomie Humaine. Descriptive, Topographique, Fonctionnelle* (Masson et Cie, Paris, France, ed. 12, 1985), pp. 244–248.

32. Y. Chen, Y. B. Park, E. Patel, G. J. Silverman, IgM antibodies to apoptosis-associated determinants recruit C1q and enhance dendritic cell phagocytosis of apoptotic cells. *J. Immunol.* **182**, 6031–6043 (2009).

33. H. M. Liu, K. Anderson, B. Caterson, Demonstration of a keratan sulfate proteoglycan and a mannose-rich glycoconjugate in corpora amylacea of the brain by immunocytochemical and lectin-binding methods. *J. Neuroimmunol.* **14**, 49–60 (1987).

34. K. S. Sfanos, B. A. Wilson, A. M. De Marzo, W. B. Isaacs, Acute inflammatory proteins constitute the organic matrix of prostatic corpora amylacea and calculi in men with prostate cancer. *Proc. Natl. Acad. Sci. U.S.A.* **106**, 3443–3448 (2009).

35. A. G. Baxter, The origin and application of experimental autoimmune encephalomyelitis. *Nat. Rev. Immunol.* **7**, 904–912 (2007).

36. R. Gold, C. Linington, H. Lassmann, Understanding pathogenesis and therapy of multiple sclerosis via animal models: 70 years of merits and culprits in experimental autoimmune encephalomyelitis research. *Brain* **129**, 1953–1971 (2006).

37. M. W. Bradbury, H. F. Cserr, R. J. Westrop, Drainage of cerebral interstitial fluid into deep cervical lymph of the rabbit. *Am. J. Physiol.* **240**, F329–F336 (1981).

38. B. Olsson *et al.*, CSF and blood biomarkers for the diagnosis of Alzheimer's disease: A systematic review and meta-analysis. *Lancet Neurol.* **15**, 673–684 (2016).

39. L. H. Meeter *et al.*, Neurofilament light chain: A biomarker for genetic frontotemporal dementia. *Ann. Clin. Transl. Neurol.* **3**, 623–636 (2016).

40. L. H. Meeter, L. D. Kaat, J. D. Rohrer, J. C. van Swieten, Imaging and fluid biomarkers in frontotemporal dementia. *Nat. Rev. Neurol.* **13**, 406–419 (2017).

41. M. Stangel *et al.*, The utility of cerebrospinal fluid analysis in patients with multiple sclerosis. *Nat. Rev. Neurol.* **9**, 267–276 (2013).

42. A. Lleó *et al.*, Cerebrospinal fluid biomarkers in trials for Alzheimer and Parkinson diseases. *Nat. Rev. Neurol.* **11**, 41–55 (2015).

43. V. Martínez *et al.*, Establishment of an in vitro photoassay using THP-1 cells and IL-8 to discriminate photoirritants from photoallergens. *Toxicol. In Vitro* **27**, 1920–1927 (2013).